

Figure 1: The figure shows our Ni isotope data for whole-rocks and mineral separates together with previously published data of peridotite reference materials. The smaller data points are published Ni isotope data are from (1, 2) Gueguen et al. (2013) and Chernonozhkin et al. (2015) (the anomalous measurement of PCC-1 by Cameron et al., 2009, is not included), (3) Steele et al. (2011), (4) Steele et al. (2011) and Chernonozhkin et al. (2015). A best estimate of the Ni isotope composition of the modern mantle is highlighted as the shaded area ($\delta^{60}\text{Ni} = 0.23 \pm 0.06$ ‰).

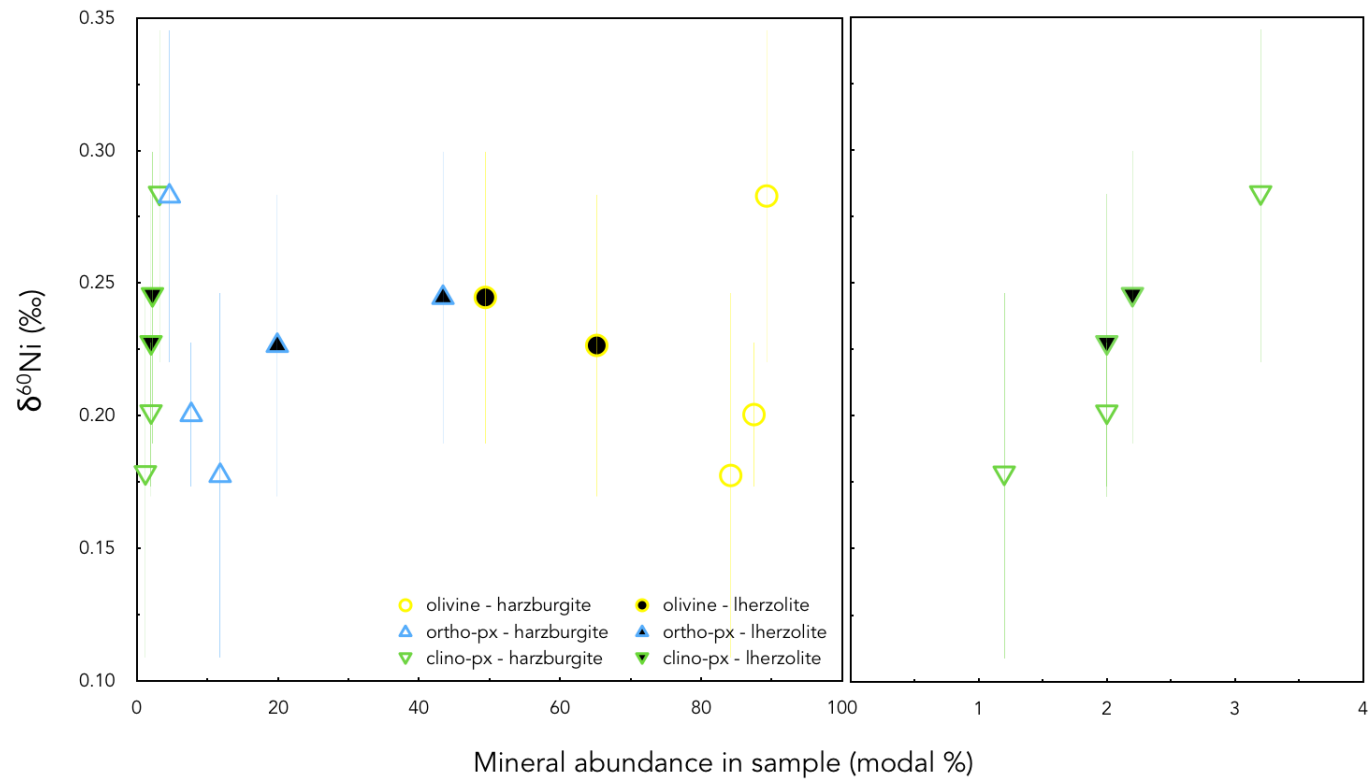


Figure 2: The figure shows the modal mineral abundances of olivine, orthopyroxene and clinopyroxene in the Tanzanian lherzolite and harzburgite xenoliths plotted against their whole-rock $\delta^{60}\text{Ni}$ values. Clinopyroxene is highlighted on the right to demonstrate that its heavy isotope composition is likely due to a larger amount of isotopically heavy clinopyroxene.

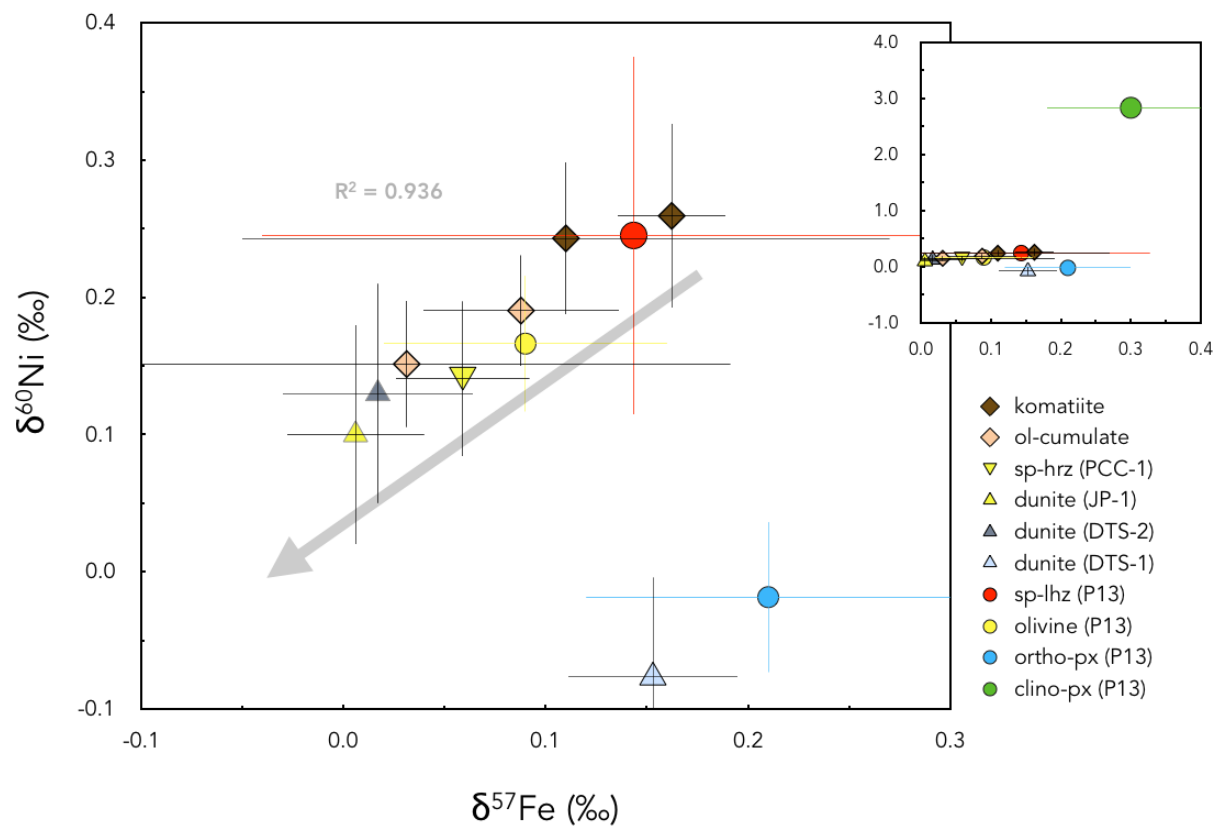


Figure 3: $\delta^{60}\text{Ni}$ plotted against $\delta^{57}\text{Fe}$ for the Gorgona samples, the peridotite reference materials PCC-1, DTS-1, DTS-2, JP-1 and the spinel lherzolite P13. Nickel isotope data for DTS-2 and JP-1 are from Steele et al. (2011). Fe isotope data for PCC-1 and DTS-2 are from Dauphas et al. (2009), for DTS-1 and JP-1 from Poitrasson et al. (2004), for P13 and its mineral separates from Williams et al. (2009), and for the komatiites and olivine cumulates from Hibbert et al. (2012). All Fe isotope data can be found in a supplemental data table.

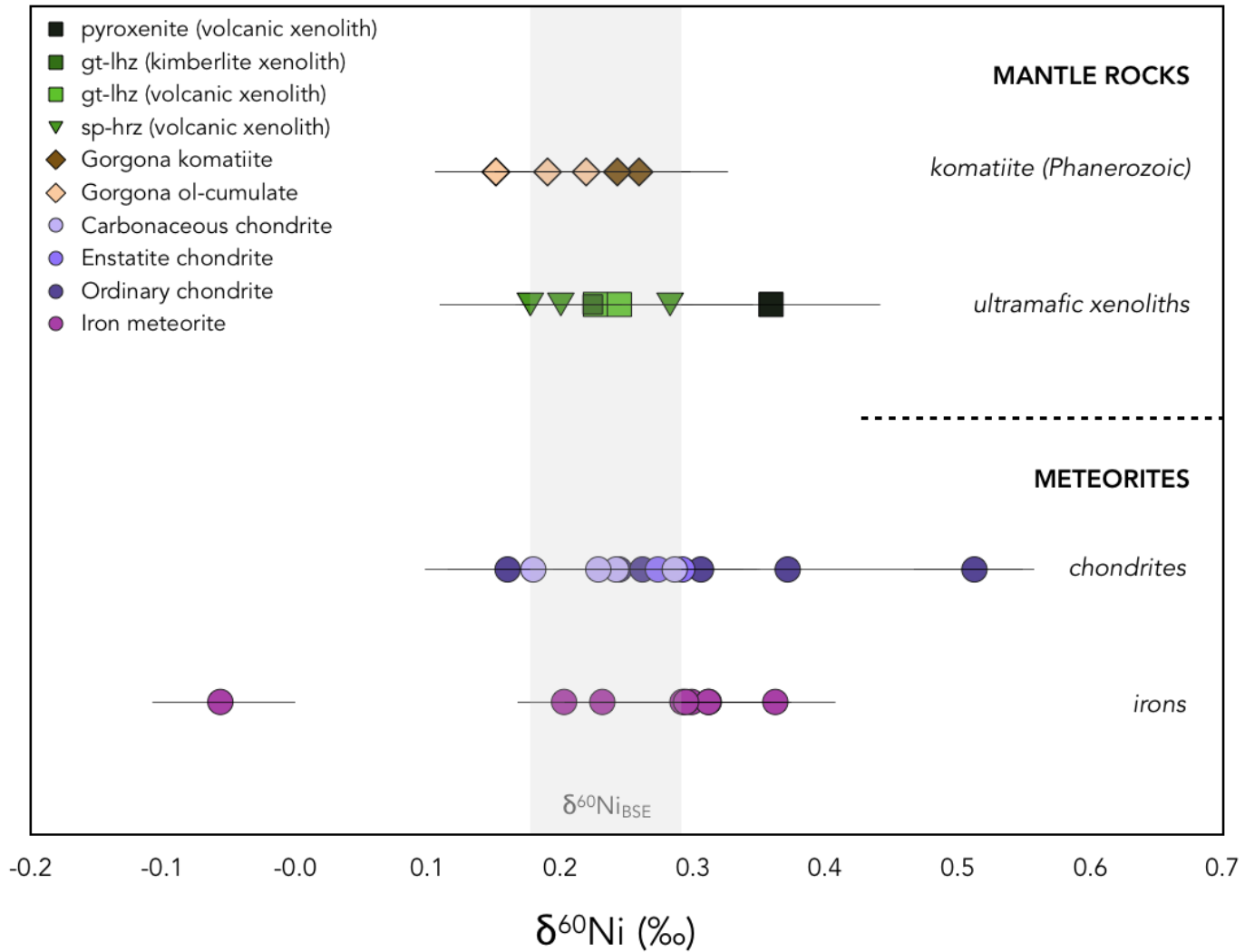


Figure 4: A summary of the Ni isotope data from mantle xenoliths, komatiites, cumulates and meteorites presented here. The Ni isotope composition of the BSE is highlighted as the shaded area ($\delta^{60}\text{Ni} = 0.23 \pm 0.06\text{‰}$).

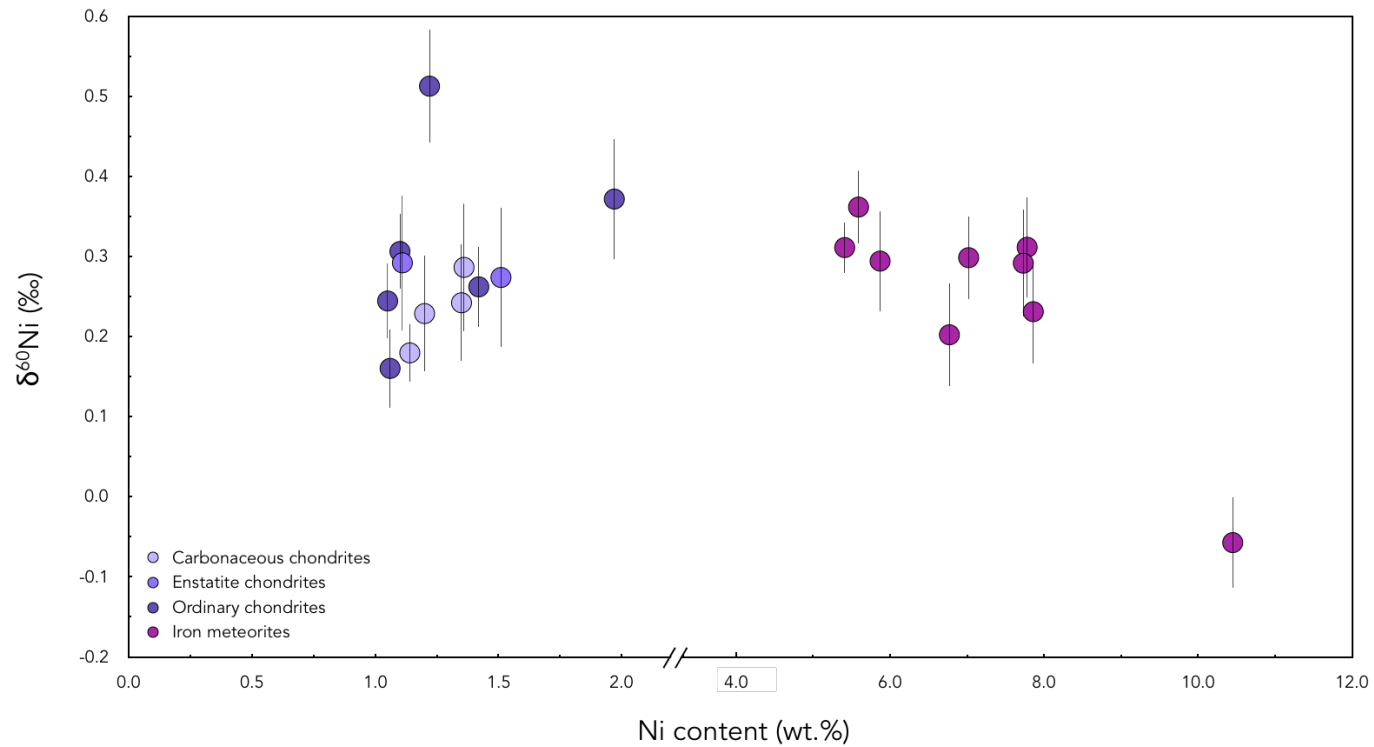


Figure 5: Nickel isotope composition plotted against the Ni content of meteorite samples analysed. The one very light iron meteorite sample (Duel Hill, -0.06‰) contains up to twice the amount of Ni compared to the other iron meteorites. Similarly, the two heavy ordinary chondrites (Kernouve, 0.37‰ , and Bruderheim, 0.51‰) plot outside the cluster of other chondrite meteorites.

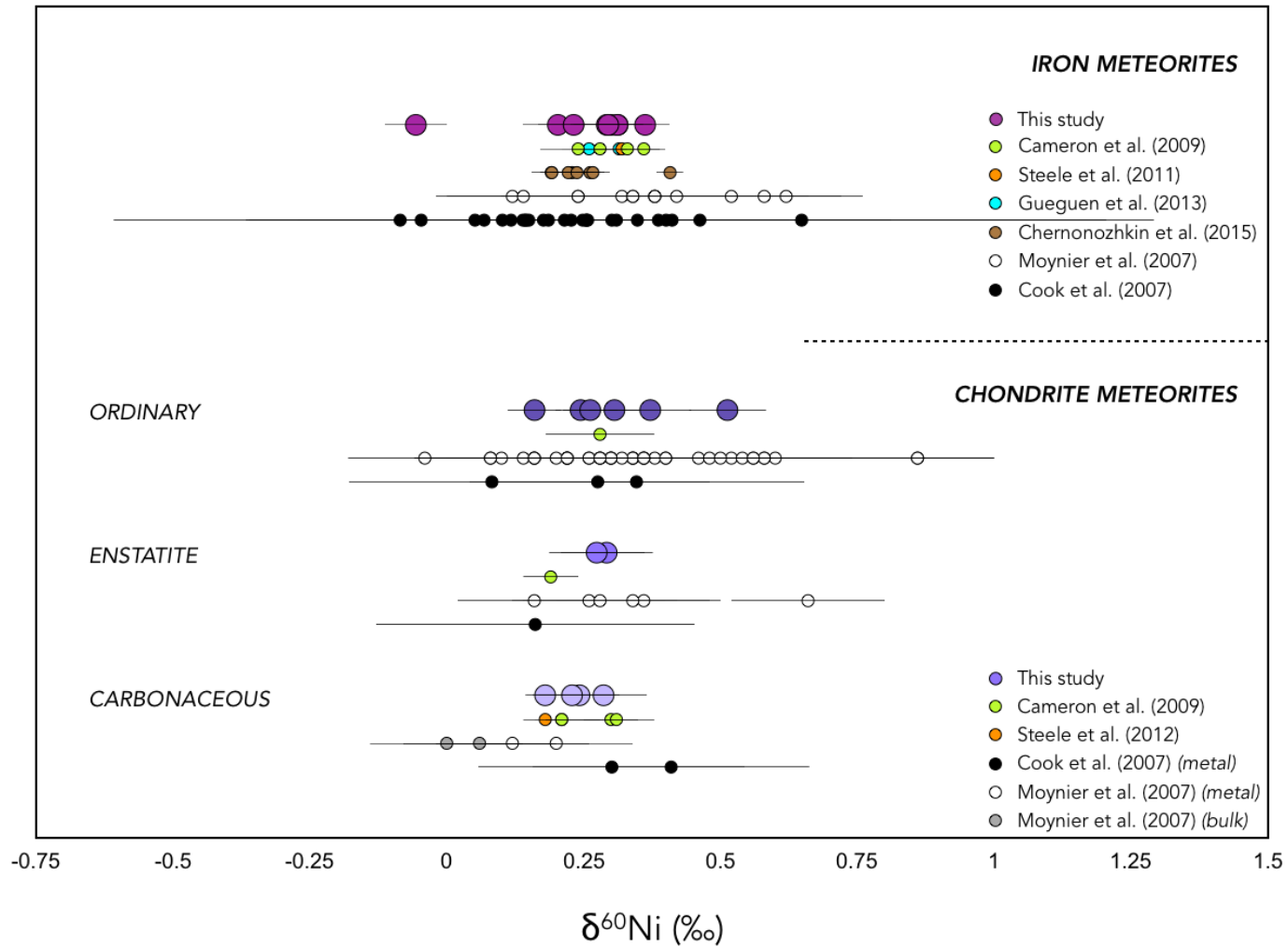


Figure 6: A comparison between meteorite data from this study and published data from Cameron et al. (2009), Steele et al. (2011, 2012), Gueguen et al. (2013), Chernozhkin et al. (2015), Moynier et al. (2007) and Cook et al. (2007). The chondrite data from Moynier et al. (2007) and Cook et al. (2007) is mostly from metal separates, not bulk samples.

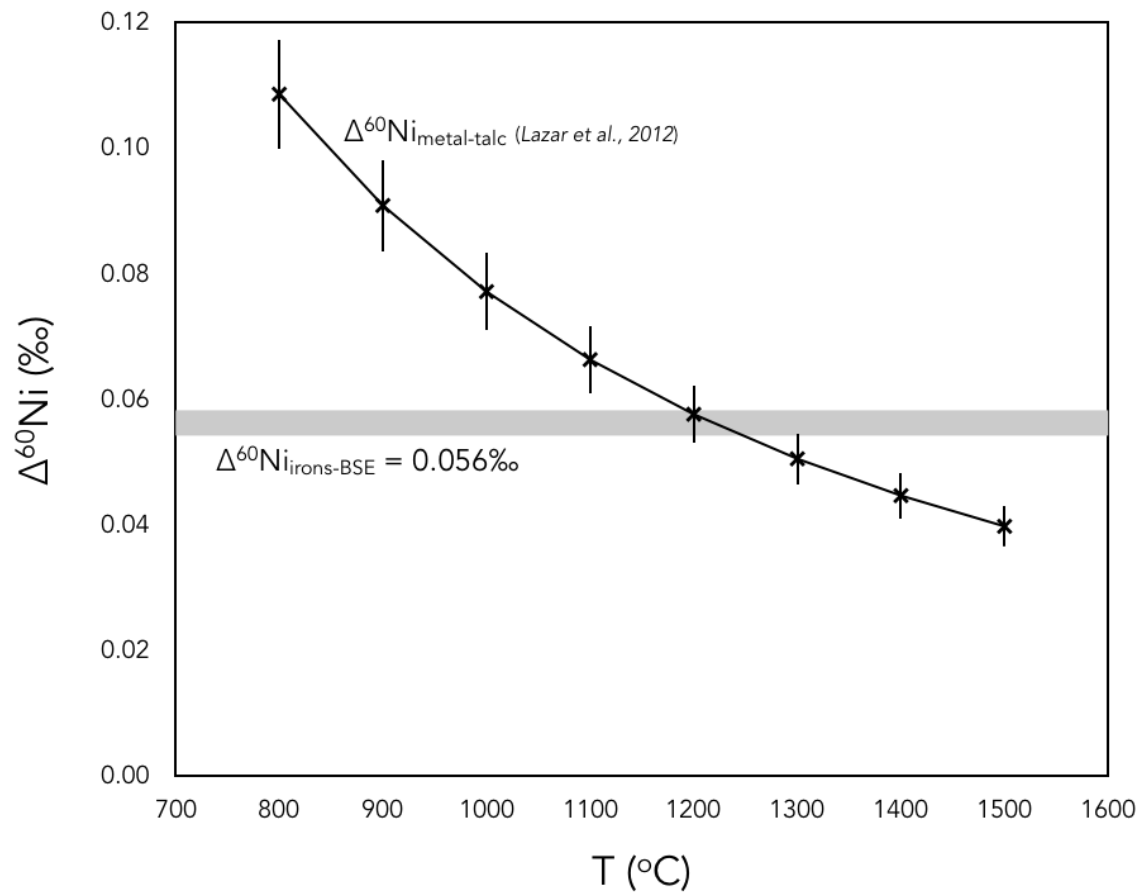


Figure 7: Nickel isotope data from metal-talc experiments by Lazar et al., 2012 suggest that Ni isotope fractionation between metal and silicate is temperature dependant, with $\Delta^{60}\text{Ni}$ being very small at normal mantle temperatures. Our data from iron meteorites and mantle rocks give an average Ni isotope fractionation between these phases of 0.056‰ ($\pm 0.06\%$; s.d.), which would put the minimum temperature these samples have been exposed to at $\sim 1200^\circ\text{C}$